http://dx.doi.org/10.5012/bkcs.2013.34.12.3829

Synthesis of Hβ (core)/SAPO-11 (shell) Composite Molecular Sieve and its Catalytic Performances in the Methylation of Naphthalene with Methanol

Xiaoxiao Wang,[†,‡] Shaoqing Guo,[§,*] and Liangfu Zhao[†,*]

[†]*Institute of Coal Chemistry, Chinese Academy of Sciences, Taiyuan 030001, P.R. China. [*]E-mail: lfzhao@sxicc.ac.cn*
[‡]*University of Chinese Academy of Sciences, Beijing 100039, P.R. China*
[§]*Taiyuan University of Science and Technology, Taiyuan 030024, P.R. China. [*]E-mail: guosq@sxicc.ac.cn*
Received August 26, 2013, Accepted September 30, 2013

Hβ (core)/SAPO-11 (shell) composite molecular sieve was synthesized by the hydrothermal method in order to combine the advantages of Hβ and SAPO-11 for the methylation of naphthalene with methanol. For comparison, the mechanical mixture was prepared through the blending of Hβ and SAPO-11. The physicochemical properties of Hβ, SAPO-11, the composite and the mechanical mixture were characterized by various characterization methods. The characterization results indicated that Hβ/SAPO-11 composite molecular sieve exhibited a core-shell structure, with the Hβ phase as the core and the SAPO-11 phase as the shell. The pore diameter of the composite was between that of Hβ and SAPO-11. The composite had fewer acid sites than Hβ and mechanical mixture while more acid sites than SAPO-11. The experimental results indicated that the composite exhibited high catalytic performances for the methylation of naphthalene with methanol.

Key Words : Hβ/SAPO-11, Synthesis, Characterization, Naphthalene methylation

Introduction

2,6-Dimethylnaphthalene (2,6-DMN) is an important intermediate in the synthesis of polyethylene naphthalate (PEN), which is a novel polyester and possesses some superior properties, such as high tensile strength, heat resistance and gas barrier property.[1,2] The synthesis of 2,6-DMN by the methylation of naphthalene with methanol over molecular sieves has aroused more attention due to its simple synthetic route and low production cost. Moreover, the products of the methylation are very complicated and dimethylnaphthalene (DMN) has 10 different isomers with similar boiling point. It is very difficult to separate 2,6-DMN from 2,7-DMN due to the very tiny difference in boiling point of only 0.3 K. Therefore, the key role of the process is to find a molecular sieve with high selectivity of 2,6-DMN at acceptable conversion of naphthalene.

Recently, the methylation of naphthalene has been studied over some molecular sieves such as ZSM-5, HY, Mordenite, SAPO-11 and Hβ.[3-7] Among them, Hβ and SAPO-11 showed relatively high performances.[4,7] Hβ was firstly synthesized in 1967. It has strong acidity and a tridimensional system of interconnected 12-membered ring channels with pore size of 0.55×0.55 nm^2 and 0.76×0.64 nm^2.[8,9] It exhibited initially high naphthalene conversion because its acidic sites are highly accessible. However, it is rapidly deactivated by coke deposition owing to its strong acidity[4,7] and showed the low selectivity of 2,6-DMN because of its wide pore diameters.[7] SAPO-11 is a member of the silico-aluminophosphate (SAPO-n) family which was firstly synthesized by Union Carbide Corporation. It presented a milder acidity and had a one-dimensional pore molecular sieve with pore size of 0.39 nm × 0.63 nm.[10,11] It exhibited higher stability due to its milder acidity and higher selectivity of 2,6-DMN due to its smaller pore diameters.[7,12] However, it showed lower initial naphthalene conversion because of its weak acidity. In summary, both Hβ and SAPO-11 are not the perfect molecular sieves for the synthesis of 2,6-DMN by the methylation of naphthalene.

Recently, binary structure composite molecular sieve has attracted more attention.[13-16] Fan *et al.*[13] synthesized aluminosilicate/silicoaluminophosphate composite of ZSM-5/SAPO-11. Compared with the mechanical mixture of ZSM-5 and SAPO-11, the composite of ZSM-5/SAPO-11 had more mesopores and moderate acidity distribution which could accelerate the diffusion of products and could be considered as a potential catalyst system for hydro-upgrading FCC gasoline. Zhang *et al.*[14] reported that the binary microporous molecular sieve composite of Y/Hβ showed higher activity and middle distillate yield in vacuum gas oil hydrocracking process because of the interface effect of the bi-phase molecular sieve in the composite. Generally speaking, the composite molecular sieve with binary structure not only combines the advantages of the two original molecular sieves, but also promotes the formation of special properties which can improve the catalytic performance. Based on this idea, the composite of Hβ and SAPO-11 should combine the advantages of Hβ and SAPO-11, leading to the high catalytic performances in the methylation of naphthalene. Therefore, the Hβ (core)/SAPO-11 (shell) composite molecular sieve was synthesized through hydrothermal method in this paper. For comparison, the mechanical mixture was prepared through the blending of Hβ with SAPO-11. The physicochemical properties of Hβ, SAPO-11, the composite and the mechanical mixture were characterized by XRD, SEM, TEM, FT-IR, N_2 adsorption-desorption and NH_3-TPD, and their cata-

lytic performances of these samples were also studied for the methylation of naphthalene with methanol.

Experimental

Catalyst Preparation. Hβ was obtained from the Catalyst Plant of Nankai University. SAPO-11 was synthesized from synthetic gel composition $1.0Al_2O_3$: $1.0P_2O_5$: $0.6SiO_2$: 1.2template : $49H_2O$. Pseudoboehmite (72 wt % Al_2O_3), orthophosphoric acid (85% H_3PO_4) and silica sol (30 wt % SiO_2) were used as source of Al, P and Si. Di-*n*-propylamine (99 wt %) was used as the template. The final crystallization temperature of 453.15 K and crystallization time of 24 h was employed. The as-synthesized samples were washed with distilled water, then dried at 393.15 K for 12 h and calcined at 873.15 K for 4 h. Hβ/SAPO-11 composite molecular sieve was synthesized *via* hydrothermal approach and the step was as follows: (1) 9.8 g of orthophosphoric acid (85% H_3PO_4) was added to 75 g of distilled water and the mixture was stirred for 30 min. Then, 5 g of Hβ powder was added to 30 mL of distilled water and stirred for 30 min to form gel A. (2) 5.6 g of pseudoboehmite (72 wt % Al_2O_3) was added dropwise and the mixture was stirred for another 30 min. Afterwards, silica sol (30 wt % SiO_2) was added dropwise with further stirring for 120 min to get a homogeneous gel B. (3) 7.2 g of di-*n*-propylamine (99 wt %) was added to the mixture of gel A and B (1:1). The mixture was stirred for 150 min to form homogenous gel C. (4) Gel C was transferred to a stainless steel autoclave and heated to 453.15 K for 24 h to produce the solid production. Then the solid production were washed with distilled water and dried at 393.15 K overnight. At last, the solid production was calcinated at 823.15 K for 6 h to remove the templates in the pores of the sample. In this way, the Hβ/SAPO-11 composite molecular sieve was obtained. For comparison, the mechanical mixture of Hβ/SAPO-11 was prepared by blending of Hβ with SAPO-11 (self-made).

Catalyst Characterization. X-ray powder diffraction (XRD) analysis was performed on RigakuD/maxrB X-ray diffractometer. Diffraction patterns were recorded with Cu Ka radiation at 40 kV and 100 mA in the scan range between 5° and 50° to identify the phase structure of the sample. The textural properties of the samples were derived from N_2 adsorption-desorption measurement on Micromeritics Tristar 3000. In each case, the sample was outgassed under vacuum at 573.15 K for 3 h before N_2 adsorption. The specific surface area (S_{BET}) was calculated according to BET method and the volume of porous (V_{pore}) was obtained by t-plot analysis of the adsorption isotherm. Scanning electron microscopy (SEM) was performed with a LEO-435VP scanning electron microscopy operated at 20 kV and 50 pA. Transmission electron microscopy (TEM) images were obtained using a JEOL JEM-2010 microscope. Fourier transform infrared spectroscopy (FT-IR) spectra were respectively recorded with a Nicolet 380 FT-IR spectrometer. The acidity was examined by temperature-programmed desorption of ammonia (NH_3-TPD) techniques. NH_3-TPD was carried out by a flow system with a thermal conductivity detector. All samples were preheated from room temperature to 773.15 K in argon flow and kept at 773.15 K for 1 h, which was followed by NH_3 saturation in a flowing NH_3/Ar stream at 313.15 K for 5 min., Evacuation at 313.15 K for 40 min was carried out to remove physically adsorbed NH_3. Then the sample was heated to 873.15 K at a linear heating rate of 10 K/min, and the detector signal of NH_3 was recorded.

Catalytic Test. The experiments were performed in a fixed-bed continuous-flow reactor equipped with 20 mm diameter and 600 mm length stainless steel tube. 2.5 g of 20-40 mesh molecular sieve catalysts were loaded in the reaction tube. The reaction mixture was fed into the reactor by a quantity measuring pump and the pressure was kept by N_2. The weight hourly space velocity (WHSV) of naphthalene was 0.19 h^{-1} in all experiments. Reactive temperature was 623.15 K and the liquid reactant including naphthalene, methanol and mesitylene (solvent) in a molar ratio of 1:5:3.5 were preheated before passing to the reactor. Reaction products were analyzed by gas chromatography (GC9560) with a Beta-Dex120 capillary column. The naphthalene conversion was calculated as follows:

$$\text{Naphthalene conv. (\%)} = \left(\frac{n_{N,0}-n_N}{n_{N,0}}\right) \times 100$$

Where $n_{N,0}$ and n_N are the molar percentage of naphthalene before and after the reaction. The selectivity of 2,6-DMN is the corresponding molar percentage in the sum of all DMN isomers. And the selectivity of other DMN is also the corresponding molar percentage in the sum of all DMN isomers. 2,6-DMN yield = (naphthalene conversion × 2,6-DMN distribution)/100%.

Results and Discussion

Characterization.

XRD: The XRD patterns of Hβ, SAPO-11, the mechanical mixture and the composite are shown in Figure 1. The typical characteristic peaks at 2θ = 7.5° and 22.4° attributing

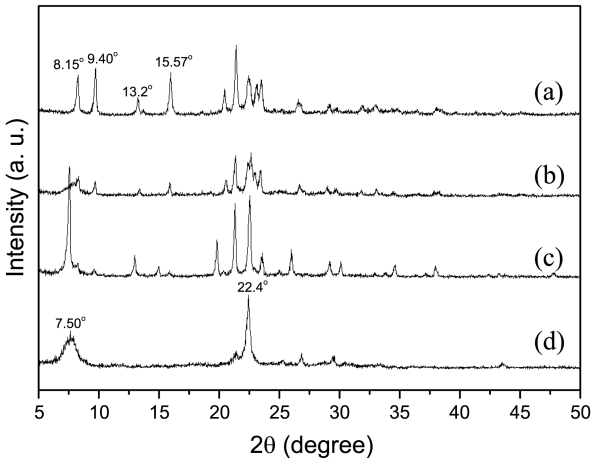

Figure 1. XRD patterns of the samples (a) SAPO-11, (b) the mechanical mixture, (c) the composite, (d) Hβ.

to Hβ[14] and peaks at 2θ = 8.15°, 9.40°, 13.2° and 15.57° attributing to SAPO-11[10] are identified for the mechanical mixture and the composite. It can be seen that the crystallinity of the composite is higher than that of the mechanical mixture. Meanwhile, the XRD peak positions slightly shifts to a lower 2θ for the composite, which is due to the formation of defects and/or lattice contraction in the framework. It implies that the interaction between SAPO-11 and Hβ can be existed in the composite.

SEM and TEM: The morphology of the samples was determined by SEM and the pictures are listed in Figure 2(a-f). Figure 2(a) shows the agglomerative crystal morphology for Hβ, whereas spherical shaped crystals are visible for SAPO-11 (see Figure 2(b) and (c)). It is clear that the mechanical mixture (see Figure 2(d)) appears two different crystal morphologies (agglomerative and spherical) for the mechanical mixture, which indicates that Hβ and SAPO-11 exist independently in the mechanical mixture. For the composite, Figure 2(e) shows a unique spherical crystal morphology which indicates that Hβ is embedded in SAPO-11. As shown in Figure 2(c) (SAPO-11) and Figure 2(f) (the composite), the morphology of SAPO-11 crystal is different from that of the composite which owns a unique core/shell structure, although they are both spherical shaped. To further understand the core/shell structure of the composite, the samples were also determined by TEM and the result is shown in Figure 3(a). It is obvious that the composite is composed of two different types of particles, with Hβ as the core, and SAPO-11 as the shell (Figure 3(a)). This is totally different

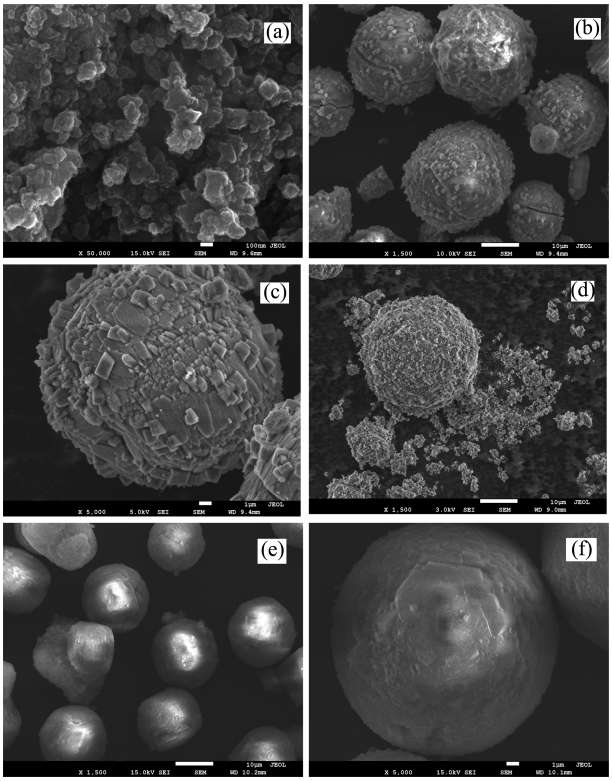

Figure 2. SEM images of the samples (a) Hβ, (b, c) SAPO-11, (d) the mechanical mixture, (e, f) the composite.

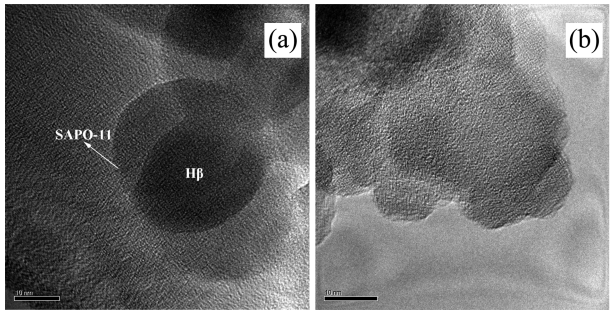

Figure 3. TEM images of the samples (a) the composite, (b) the mechanical.

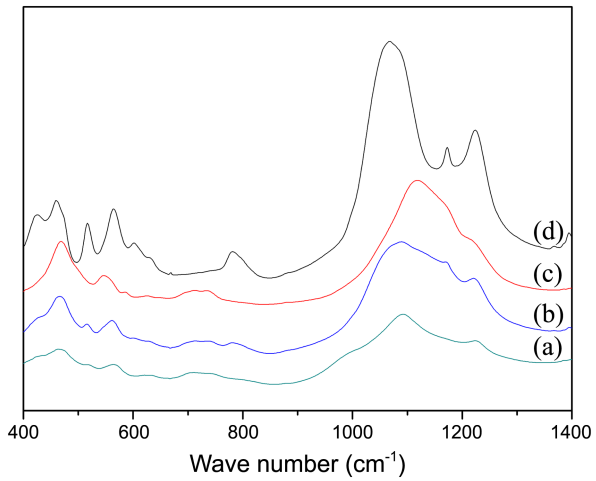

Figure 4. FT-IR spectra of the samples (a) the composite, (b) the mechanical mixture, (c) SAPO-11, (d) Hβ.

from the TEM images of the mechanical mixture (Figure 3(b)). These results indicate that Hβ and SAPO-11 are combined more uniformly in the composite than in the mechanical mixture.

FT-IR: The FT-IR spectra of the four samples are shown in Figure 4. IR bands in the range of 400-1300 cm^{-1} are due to the vibration of the molecular sieve framework. The assignment of IR bands, as presented in Table 1, shows that the composite and the mechanical mixture almost have all characteristic peaks which could be attribute to Hβ and SAPO-11. Compared with the mechanical mixture, the shift of corresponding IR bands is found for the composite, which is due to the interfacial interactions between the two phases in the composite.[17] Meanwhile, the peak at 781 cm^{-1} for the mechanical mixture, standing for the symmetric vibration of tetrahedra outer links in Hβ,[18] disappears in the composite. According to Liu *et al.*'s report,[18] the symmetric vibration of

Table 1. Position of the observed IR bands on the samples samples

Sample	Wave number (cm^{-1})						
Hβ	1224	1173	782		–	546	466
SAPO-11	–	1118	–	712	625	566	466
The composite	1223	1092	–	711	620	563	466
mechanical mixture	1220	1089	781	713	–	561	466

Table 2. Pore structure parameters of the samples

Sample	S_{BET}[a] /(m^2/g)	Total Pore volume[b] /(cm^3/g)	Pore diameter[c] /(nm)
Hβ	340	0.310	0.76
SAPO-11	149	0.145	0.63
composite	199	0.157	0.65
mechanical mixture	233	0.185	0.70

[a]BET method. [b]*t*-plot method. [c]Horvath-Kawazoe method.

tetrahedra outer links is sensitive to any change in molecular sieve structure. Therefore, the disappearance of the peak at 781 cm^{-1} in the composite may attribute to a particular conjunction form of tetrahedrons and a special skeleton structure at the interface which is absent in the mechanical mixture. It suggests that there are strong interactions between SAPO-11 and Hβ in the composite.

N_2 Isothermal Adsorption-Desorption Characterization. The textural properties of the samples were characterized by N_2 isothermal adsorption-desorption and the result is listed in Table 2. As shown in Table 2, Hβ owns the maximum S_{BET} while SAPO-11 owns the minimum S_{BET}. The mechanical mixture shows higher S_{BET} than the composite does. The total pore volume and pore diameter of the samples gradually decrease as the following sequence of Hβ > the mechanical mixture > the composite > SAPO-11. The composite has smaller S_{BET} and less pore volume than Hβ and the mechanical mixture. Compared with SAPO-11, the pore diameter of the composite is larger, which indicates that Hβ is introduced into SAPO-11 during the synthesis process. It should be noted that the pore diameter of the composite is smaller than that of the mechanical mixture, which further indicates that SAPO-11 and Hβ have strong interaction in the composite.

NH_3-TPD. The acidic properties were characterized by NH_3-TPD for the investigated samples. The acid strength was determined by the ammonia desorption peak temperature, while the acid amount was estimated by the areas under the TPD curves. The results of NH_3-TPD in Figure 5 show that

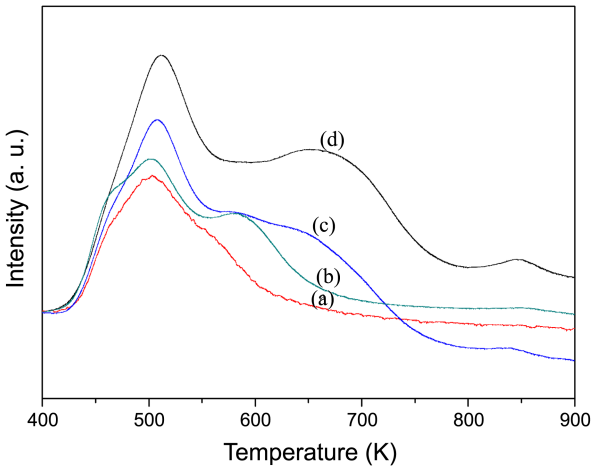

Figure 5. NH_3-TPD profiles of the samples (a) SAPO-11, (b) the composite, (c) the mechanical mixture, (d) Hβ.

Hβ has the strongest acidity, while SAPO-11 has the weakest acidity. The mechanical mixture shows medium acidity, which nearly equals to the average acidity of Hβ and SAPO-11. Compared with the mechanical mixture, the composite exhibits lower acidity, which further indicates the occurrence of strong interaction of Hβ and SAPO-11 in the composite. As shown in Figure 5, the acid strength and the total acid amount of the acidic sites decreases in the order of Hβ > the mechanical mixture > the composite > SAPO-11. As discussed above, Hβ is covered by the SAPO-11 in the composite (see Figure 2), which leads to lower acidity for the composite than that for Hβ and the mechanical mixture. Meanwhile, the composite exhibits lower acidity than SAPO-11, which is probably attributed to the core (Hβ)/shell (SAPO-11) structure of the composite.

Formation Mechanism of Hβ (core)/SAPO-11 (shell) Composite. Based on the above discussion, it is found that the physicochemical properties of the composite are different from those of the mechanical mixture, which is related to its formation mechanism. As stated above, the mechanical mixture is just prepared through the blending of Hβ and SAPO-11, resulting in the existence of Hβ and SAPO-11 independently. However, the composite is synthesized *via* hydrothermal method, resulting in the Hβ (core)/SAPO-11 (shell) structure in the composite. The possible formation mechanism of Hβ (core)/SAPO-11 (shell) composite is put forward as follows. First, as one of raw material of SAPO-11, orthophosphoric acid combines with Hβ by chemical bond and the Hβ is fixed in this way. Then, orthophosphoric acid reacts with pseudoboehmite and silica sol to form the colloid (containing Al, P and Si) around the Hβ. At last, di-*n*-propylamine (template) is added to the colloid and reacts with it to form SAPO-11 crystals around Hβ. Generally, Hβ serves as a seed for the crystallization of the composite during the synthesis process of the composite. Thus, the interaction existed in the SAPO-11 and Hβ maybe refer to the chemical bond between orthophosphoric acid and Hβ.

Catalytic Performances. The catalytic performances of the investigated samples with 1 h and 6 h time on stream (TOS) are listed in Table 3. The conversion of naphthalene decreases in the order of the composite > SAPO-11 > the mechanical mixture > Hβ at 6 h of TOS although it decreases in the order of Hβ > the mechanical mixture > the composite > SAPO-11 at 1 h of TOS. Also, the composite shows the

Table 3. Comparison of catalytic performance of the samples

	Time	Hβ	SAPO-11	Composite	Mechanical
Naphthalene conv (%)	1 h	63.2	55.2	57.2	58.6
	6 h	10.6	32.5	29.3	20.5
Selectivity of 2,6-DMN	1 h	23.6	23.9	26.2	23.5
	6 h	8.3	30.4	38.2	15.6
2,6-DMN yield%	1 h	4.94	6.96	7.85	5.46
	6 h	1.09	3.50	4.62	2.32

Reaction conditions: Temperature = 350 °C, Pressure = 0.1 MPa, WHSV = 0.19 h^{-1}, naphthalene:methanol:mesitylene = 1:5:3.5 (molar ratio), time-on-stream = 1 h, 6 h.

highest selectivity of 2,6-DMN and the highest 2,6-DMN yield over the investigated samples. These results indicate that the composite exhibits high catalytic performance in the methylation of naphthalene than the mechanical mixture, Hβ and SAPO-11 with time prolonged.

As shown in Table 3, Hβ presents the highest conversion of naphthalene (63.2%) at 1 h of TOS and the lowest conversion of naphthalene (10.6%) at 6 h of TOS .The conversion of naphthalene for SAPO-11 is 55.2% and 32.5% at the reaction time of 1 h and 6 h, respectively. The naphthalene conversion of mechanical mixture is 58.6% at 1 h of TOS but decreases to 20.5% at 6 h of TOS. The conversion of naphthalene for the composite is 57.2% at 1 h of TOS and 29.3% at 6 h of TOS. In general, SAPO-11 has the highest stability and Hβ has the lowest stability among the samples for the reaction. The stability of the composite is higher than that of the mechanical mixture. As mentioned above, Hβ has the strongest acidity, while SAPO-11 has the weakest acidity. It is generally accepted that the strong acid sites can accelerated the formation of coking, leading to the catalyst deactivation. Therefore, the low stability of Hβ might be caused by its high concentration of strong acid sites while the high stability of SAPO-11 might be caused by its weak acidity. Also, the stability of the composite and the mechanical mixture is consistent with their acidity. As stated previously, the composite has less acidity than the mechanical mixture. So the stability of the composite is higher than that of the mechanical mixture. Generally, the higher the acidity is, the lower the stability becomes.

Table 3 shows that the selectivity of 2,6-DMN decreases in the order of the composite > SAPO-11 > the mechanical mixture > Hβ, which does not agree with the acidity of four samples. This indicates that the selectivity of 2,6-DMN has no clearly relationship with the acidity of samples. However, it has relationship with the pore size of samples. The distributions of ten DMN isomers of the methylation of naphthalene over four samples at 6 h of TOS (see Figure 6) show that 2,6-DMN over SAPO-11 and the composite is dominant, which is possibly because of the steric hindrance effect. The pore size of SAPO-11 (0.63 nm) and the composite (0.65 nm) are favorable to produce 2,6-DMN (0.64 nm)[19] because the molecule size of 2,6-DMN is similar to the pore size of SAPO-11 and the composite. Figure 6 also shows that 2,7-DMN and 2,3-DMN over Hβ and the mechanical mixture are dominant. It seems that the relatively large-sized DMN isomers should be dominant over Hβ and the mechanical mixture because of the large pore size of Hβ (0.76 nm) and the mechanical mixture (0.70 nm). However, the results in Figure 6 show that the relatively small-sized 2,7-DMN and 2,3-DMN are the main products. Actually, the relatively large-sized DMN isomers are formed in the pore channels at first during the synthesis process. However, they can block easily the pores channels of Hβ and the mechanical mixture, preventing the further diffusion of the relatively large-sized DMN isomers. Thus, the relatively small-sized 2,7-DMN and 2,3-DMN could easily diffuse out of the pores channels of them.

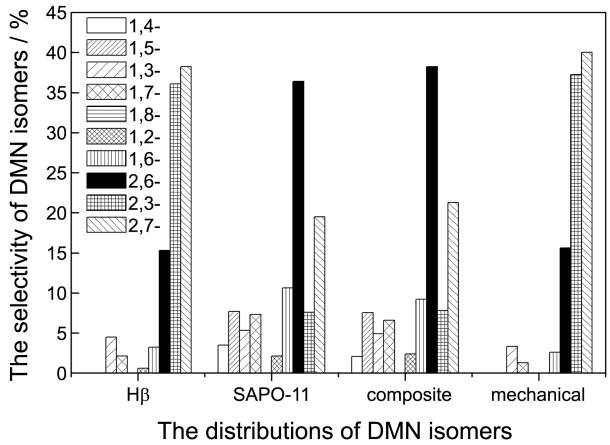

Figure 6. The distributions of DMN isomers in the methylation of naphthalene with 6 h time on stream.

It should be noted that the selectivity of 2,6-DMN over the composite is higher than that over SAPO-11 although 2,6-DMN over the composite and SAPO-11 is dominant (see Table 3 and Figure 6). Because the molecule size of 2,6-DMN (0.64 nm) is larger than the pore size of SAPO-11 (0.63 nm) and smaller than the pore size of the composite (0.65 nm), 2,6-DMN suffers more diffusion resistance in the relatively narrow pore channels of SAPO-11 than that in the relatively broader pore channels of the composite, leading to the relatively lower selectivity of 2,6-DMN over SAPO-11 and the relatively higher selectivity of 2,6-DMN over the composite.

Conclusion

Hβ (core)/SAPO-11 (shell) composite molecular sieve could be synthesized by the hydrothermal method and applied to the methylation of naphthalene with methanol. The characterization results showed that Hβ/SAPO-11 composite molecular sieve exhibited a core-shell structure, with the Hβ phase as the core and the SAPO-11 phase as the shell. The pore diameter of the composite was helpful for the diffusion of 2,6-DMN, leading to a higher selectivity of 2,6-DMN and the higher 2,6-DMN yield. Meanwhile, the composite showed relatively higher stability. In general, the Hβ/SAPO-11 composite molecular sieve showed high catalytic performances in the methylation of naphthalene with methanol, which was closely bound up to the interaction exist in the SAPO-11 and Hβ in the composite. The results also shed light on the design of novel composite catalysts towards the methylation of naphthalene and other applications.

Acknowledgments. This work was supported by the National High-tech R&D Program of China (863 Program) (2012AA051002). And the publication cost of this paper was supported by the Korean Chemical Society.

References

1. Song, C.; Schobert, H. H. *Fuel. Process. Technol.* **1999**, *33*, 157.

2. Tsutsui, T.; Ijichi, K.; Inomata, T.; Kojima, T.; Sato, K. *Chem. Eng. Sci.* **2004**, *59*, 3993.
3. Fraenkel, D.; Cherniavsky, M.; Ittah, B.; Levy, M. *J. Catal.* **1986**, *101*, 273.
4. Park, J. N.; Wang, J.; Lee, C. W.; Park, S. E. *Bull. Korean Chem. Soc.* **2002**, *23*, 1011.
5. Pazzuconi, G.; Terzoni, G.; Perego, C.; Bellussi, G. *Stud. Surf. Sci. Catal.* **2001**, *135*, 4071.
6. Bai, X. F.; Sun, K. Y.; Wu, W.; Yan, P. F.; Yan, J. *Appl. Catal. A* **2010**, *375*, 279.
7. Wang, X. X.; Zhang, W.; Guo, S. Q.; Zhao, L. F.; Xiang, H. W. *J. Brazil. Chem. Soc.* **2013**, *24*, 1180.
8. Treacy, M. M. J.; Newswam, J. M. *Nature* **1988**, *332*, 249.
9. Higgins, J. B.; Lapierre, R. S.; Schlenker, J. L.; Rohrman, A. C.; Wood, J. D.; Keller, G. T.; Rohrbaugh, W. J. *Zeolites* **1988**, *8*, 446.
10. Lok B. M.; Messina, C. A.; Patton, R. L.; Gajek, R. T.; Cannon, T. R.; Flanigen, E. M. *Crystalline Silicoaluminophosphates*, US. 4440871. 1984.
11. Song, C. M.; Feng, Y.; Ma, L. L. *Micropor. Mesopor. Mat.* **2012**, *147*, 205.
12. Wang, X. X.; Wen, J.; Zhang, W.; Zhao, L. F.; Wei, W. *Petro. Tech.* **2012**, *41*, 1284.
13. Fan, Y.; Lei, D.; Shi, G.; Bao, X. J. *Catal. Today* **2006**, *114*, 388.
14. Zhang, X. W.; Guo, Q.; Qin, B.; Zhang, Z. Z.; Ling, F. X.; Sun, W. F.; Li, R. F. *Catal. Today* **2010**, *149*, 212.
15. Wang, S.; Dou, T.; Li, Y. P.; Zhang, Y.; Li, X. F.; Yan, Z. C. *Catal. Commun.* **2005**, *6*, 87.
16. Zhang, Y. H.; Liu, Y. C.; Li, Y. X. *Appl. Catal. A* **2008**, *345*, 73.
17. Karlsson, A.; Stöcker, M.; Schmidt, R. *Micropor. Mesopor. Mat.* **1999**, *27*, 181.
18. Liu, S. T.; Bao, J.; Wei, W. S.; Shi, G. *Micropor. Mesopor. Mat.* **2003**, *66*, 117.
19. Fang, Y. M.; Hu, H. Q. *Catal. Commun.* **2006**, *7*, 264.